Cement & Concrete Composites 31 (2009) 637–646

Contents lists available at ScienceDirect

Cement & Concrete Composites

journal homepage: www.elsevier.com/locate/cemconcomp

Comparison of observed and simulated cement microstructure using spatial correlation functions

S. Igarashi [a,*], W. Chen [b,1], H.J.H. Brouwers [b]

[a] Department of Civil Engineering, Kanazawa University, Kakuma-machi, Kanazawa 920-1192, Japan
[b] Department of Civil Engineering, University of Twente, P.O. Box 217, 7500 AE Enschede, The Netherlands

ARTICLE INFO

Article history:
Received 6 November 2008
Received in revised form 24 June 2009
Accepted 30 June 2009
Available online 4 July 2009

Keywords:
Back-scattered-electron imaging
Microstructure
Cement paste
Modeling
Second-order statistics
Spatial set

ABSTRACT

The microstructure of cement pastes, as revealed by SEM-BSE image analysis, was compared with a simulated structure generated by the University of Twente version of the CEMHYD3D hydration simulation model. The spatial array of unhydrated cement particles was simulated by the model. However, spatial features in capillary pore structure obtained by the simulation are different from the observed microstructure. This disagreement in the spatial structure is to be expected since there are fundamental differences in porosity as represented by the two methods. Only coarse pores are detected in the SEM examination while the total capillary porosity and its whole spatial distribution are virtually simulated in the model. A subset of the visible pores must be different in spatial statistics from the universal set of total porosity. Care must therefore be taken in interpreting agreement between simulation output and microscopically observed microstructure in images.

1. Introduction

For the purposes of understanding microstructure and properties of concrete, computer simulation techniques have been developed taking advantage of the rapid advancement of computer technology [1]. Several sophisticated simulation models have been proposed for representing the formation of characteristic microstructure in cement-based materials [2–5]. Furthermore, time-series simulation of the durability of concrete structures has recently become possible, at least to some degree [6]. Computer simulation may become a general tool for investigating properties of concrete in the near future. On the other hand, all simulation models are built on assumptions and prerequisites. It is therefore important to validate the simulation results through comparisons with actual microstructure.

Diamond [7] has visually compared actual images of cement paste microstructure with the results of several simulation models in full detail. He has pointed out that those models cannot represent some significant characteristics of the actual microstructure. For example, the study revealed that random packing, which is usually assumed for cement particles in the models, is not always correct in actual concrete. This suggests that the real microstructure is more heterogeneous than the simulation output, so that a much larger region must be simulated for accurate representation of the microstructure. In Diamond's study, however, the differences between actual and simulated microstructures were deduced from qualitative observation, rather than through quantitative evaluation. The required capabilities of the models depend on their intended use. Whereas it is not reasonable to expect perfect reproduction of microstructure from the present models, there are opportunities to improve such models and their abilities to represent important features of actual cement microstructure.

Second-order stereology or spatial correlation functions are commonly used in quantitative evaluation of morphology and spatial arrays of phases in random heterogeneous microstructures [8]. The correlation function enables the understanding of geometrical differences in terms of probability in metric space. For example, Bentz [9] has used the spatial functions to compare real cement paste microstructures as revealed by X-ray computer tomography with simulated ones. He has mentioned that the results of CEMHYD3D simulation for an age of 137 h were in good agreement with the real microstructure for a 0.45- water/cement ratio paste cured under sealed conditions. CEMHYD3D is a promising, widely used simulation tool in computational materials science of concrete. However, few studies have quantitatively compared simulated structures with real structures revealed by imaging techniques such as scanning electron microscopy (SEM), which has higher resolution than the simulation generally used.

The purpose of this study is to quantitatively compare a simulated microstructure with a real one as revealed by

* Corresponding author. Tel./fax: +81 76 2646364.
E-mail address: igarashi@t.kanazawa-u.ac.jp (S. Igarashi).
[1] Present address: Wuhan University of Technology, Wuhan, Hubei, China.

0958-9465/$ - see front matter © 2009 Elsevier Ltd. All rights reserved.
doi:10.1016/j.cemconcomp.2009.06.008

back-scattered-electron (BSE) image analysis, which has finer resolution than the simulation. Cement paste specimens were produced, and cured in water. Their BSE images at prescribed ages were compared with sections of the simulated 3-D structure, which was obtained as a result of equivalent curing conditions. Some correlation functions of second-order stereology are used for a quantitative comparison of the spatial structure of the constituent phases in the cement pastes. Disagreement between the functions for the simulated and observed microstructures is related to visible differences in their geometrical characteristics. Furthermore, essential discrepancy in making comparison and finding similarity between them is discussed based on a simple finite set theory for the spatial constituent phases in cement pastes.

2. Experiments and computations

2.1. Materials and mix proportion of cement pastes

The cement used was an ordinary Portland cement with a Blaine fineness value of 331 m^2/kg. The cement compounds and its chemical compositions are given in Tables 1 and 2, respectively. The water/cement ratio in this study was 0.40. Cylindrical specimens of 100 mm in length and 50 mm in diameter were produced in accordance with JIS R5201 [10]. They were demolded at 24 h after casting, and then cured in water at 20 °C until the prescribed ages.

2.2. BSE image analysis

At the prescribed ages, slices about 10 mm thick were cut from the cylinders for the BSE image analysis. They were dried by ethanol replacement and vacuum drying, and then impregnated with a low viscosity epoxy resin. After the resin hardened at room temperature, the slices were finely polished with SiC papers. The polished surfaces were meticulously finished with a diamond slurry for a short time.

Samples were examined using an SEM (Acceleration voltage: 25 kV) equipped with a quadruple backscatter detector. The BSE images were acquired at a magnification factor of 500×. Taking account of statistical variations in the results of image analysis [11], ten fields in each specimen were randomly chosen and analyzed. Each BSE image consists of 1148 × 1000 pixels. The size of one pixel is thus about 0.22 μm × 0.22 μm. For instance, if the size of 2.5 nm is assumed as the lower limit of size for capillary pores [12], fine pores whose sizes are in the range from 2.5 nm to 0.22 μm are missing in the BSE images. Thus, the pores tallied in the image analysis can be termed "coarse capillary pores". A dynamic threshold method was used to make a binary segmentation based on the gray level histogram [13]. In this method, information on the contrast of eight neighbour pixels is also used in determining the threshold for each pixel [13]. Pixels for residual unhydrated cement particles (the brightest areas) and for pores (the darkest areas) were counted in order to obtain the area fractions of these two phases. Using the Delesse rule in model-based stereology, the area fractions of a phase in 2-D cross sections are assumed to be equal to its 3-D volume fractions [14]. The degree of hydration of cement (α) was calculated with the following equation [15,16]:

$$\alpha = 1 - \frac{UH_i}{UH_0(1 - V_{sol})} \quad (1)$$

UH_i area fraction of unhydrated cement particles at the age of t_i, UH_0 initial area fraction of unhydrated cement particles (i.e. $t_i = 0$), V_{sol} initial volume fraction of readily soluble phase (≈0.05 in the cement used in this study).

Table 1
Phase composition of the employed cement (in m/m%).

C_3S	C_2S	C_3A	C_4AF	Total
62.2%	12.1%	9.68%	7.42%	91.4%

Table 2
Oxide composition of the employed cement (in m/m%).

Ig. Loss	SiO_2	Al_2O_3	Fe_2O_3	CaO	MgO	SO_3	Na_2O	K_2O	Cl
1.19	20.55	5.21	2.44	65.86	0.91	2.33	0.27	0.41	0.006

2.3. Computer simulation

To simulate the microstructure of the cement paste, the latest University of Twente (UT) version of the computer model CEMHYD3D was used [17]. This model is primarily based on CEMHYD3D version 1.0 that was developed at NIST [3]. The UT model is modified from the original CEMHYD3D that simulates the processes of cement hydration and the formation of microstructure [18]. The UT version is an extension and can for instance simulate diffusion-controlled processes during cement hydration and minimize the influence of system resolution on the model predictions. Furthermore, it allows variations in the composition of the hydration products. It can thus simulate the hydration and microstructure development of cement pastes with additional supplementary materials (slag, fly ash, silica fume, etc.) [17,19]. The model is still operated on a cycle basis of three different steps. They are described as dissolution, diffusion and reaction (precipitation/nucleation). A time conversion factor is used to relate the hydration cycles to real time. It is proven that the new CEMHYD3D UT version is robust in regard to the time conversion factor, indicating that most of the important kinetic factors of the cement hydration process are successfully considered in the computer model [18,19].

The resolution of the simulation was normally 1 μm. A 3-D microstructure of 100 × 100 × 100 μm^3 was represented in the simulation. Ten images of 2-D cross sections were randomly obtained from the simulated 3-D structure. Those cross sections were compared with the BSE images in terms of second-order stereology. The particle size distribution which was measured by laser diffraction is given in Fig. 1. This information was used as input data for the initial placement of cement particles in the simulation. The condition for the execution of the simulation is curing in water at 20 °C. The time conversion factor used in the simulation is 3.8×10^{-3} h/cycle[2].

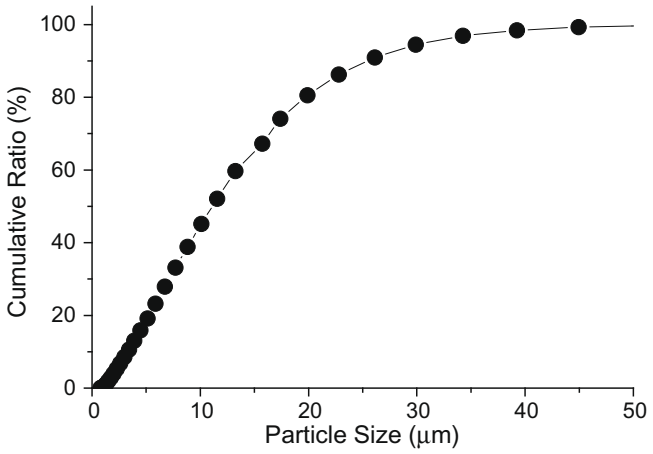

Fig. 1. Cumulative particle size distribution of the employed cement.

2.4. Two-point correlation function [8]

It is assumed that hardened cement paste consists of three regions; a hydrated matrix phase Ω_m, an unhydrated cement particle phase Ω_c, and a capillary pores phase Ω_{cp}. If a phase of interest is expressed by Ω_P, then, the following indicator function $I^{(P)}(x_i)$ is introduced;

$$I^{(P)}(x_i) = \begin{cases} 1 & (x_i \in \Omega_P) \\ 0 & (x_i \notin \Omega_P) \end{cases} \quad (2)$$

where a position vector $x_i \in (\bar{\Omega}_P \cup \Omega_P) = (\Omega_c \cup \Omega_{cp} \cup \Omega_m)$. For example, if the unhydrated cement phase is of interest, i.e. $\Omega_P = \Omega_c$, then $\bar{\Omega}_P = \Omega_m \cup \Omega_{cp}$. Then, the two-point correlation function $S_2^{(P)}(r)$ for the phase Ω_P is defined as follows [8]:

$$S_2^{(P)}(r) = \langle I^{(P)}(x_i) I^{(P)}(x_j) \rangle = P\{I^{(P)}(x_i) = 1, I^{(P)}(x_j) = 1\} \quad (3)$$

where, $P\{I^{(P)}(x_i) = 1, I^{(P)}(x_j) = 1\}$ is a probability that the two endpoints of the position vectors hit the same phase Ω_P, and the distance between two positions is defined as $r = |x_i - x_j|$. The bracket < > means expectation. Theoretically, the initial value of the two-point function (i.e. $S_2^{(P)}(0)$) is the volume fraction (V_P) of the phase, and the asymptotic value of the function (i.e. $S_2^{(P)}(r); r \to \infty$) is the square of the volume fraction (V_P^2). The distance at which the function decays to the asymptotic value for the first time is a length which characterizes the spatial distribution structure. It is called a structure or correlation distance. The distance is regarded as a length scale for positive correlation between two points selected randomly. In other words, the probability that the two points hit the phase of interest is greater than that of a Poisson distribution for a completely random structure [14].

Extending the two-point function, the lineal-path function $L_2^{(P)}(r)$ is also defined as follows [8]:

$$L_2^{(P)}(r) = \langle I^{(P)}(x_1) \cdots I^{(P)}(x_j) \cdots I^{(P)}(x_n) \rangle = P\{I^{(P)}(x_1) = 1, \ldots I^{(P)}(x_j) = 1, \ldots I^{(P)}(x_n) = 1\} \quad (4)$$

$L_2^{(P)}(r)$ is a probability that a line segment of length r is fully on the phase Ω_P when it is thrown randomly on the sample. In this case, the length $r = |x_1 - x_n|$, x_j is a point on the line segment between x_1 and $x_n (1 \leqslant j \leqslant n; j = 1, 2, \cdots, n)$.

In short, the function $S_2^{(P)}(r)$ reflects the average size and shape of the phase, and gives information on general features of the system of dispersion. On the other hand, $L_2^{(P)}(r)$ gives rough information on connectivity of the phase P of interest.

Several algorithms have been proposed for the calculation of correlation functions. In this study, a template with eight radial directions was used for the BSE images. As shown in Fig. 2a, the template was arbitrary placed on a binary image, in which phases of interest were extracted by image processing. Whether both the endpoints hit the same phase or not, was determined by numerical operations. Then the template was moved to a different grid-point. Placing the template at different locations was repeated to obtain sufficient samples statistically for a specific length r in an image. Then the radial length r was changed by some pixels, and the same procedure as explained above was repeated. As for the lineal-path function, whether the whole radial line segment was on the same phase or not was determined. On the other hand, the simulated structure is not so large in this study, as mentioned above. Therefore, instead of the radial template, horizontal and vertical grid lines were used for minimizing the edge effect on the counting procedure. Line segments with a specific length were put at random locations on those grid lines (Fig. 2b). Then, probability that two endpoints of the segment probe hit the phase of interest was calculated by the numerical operations on the image.

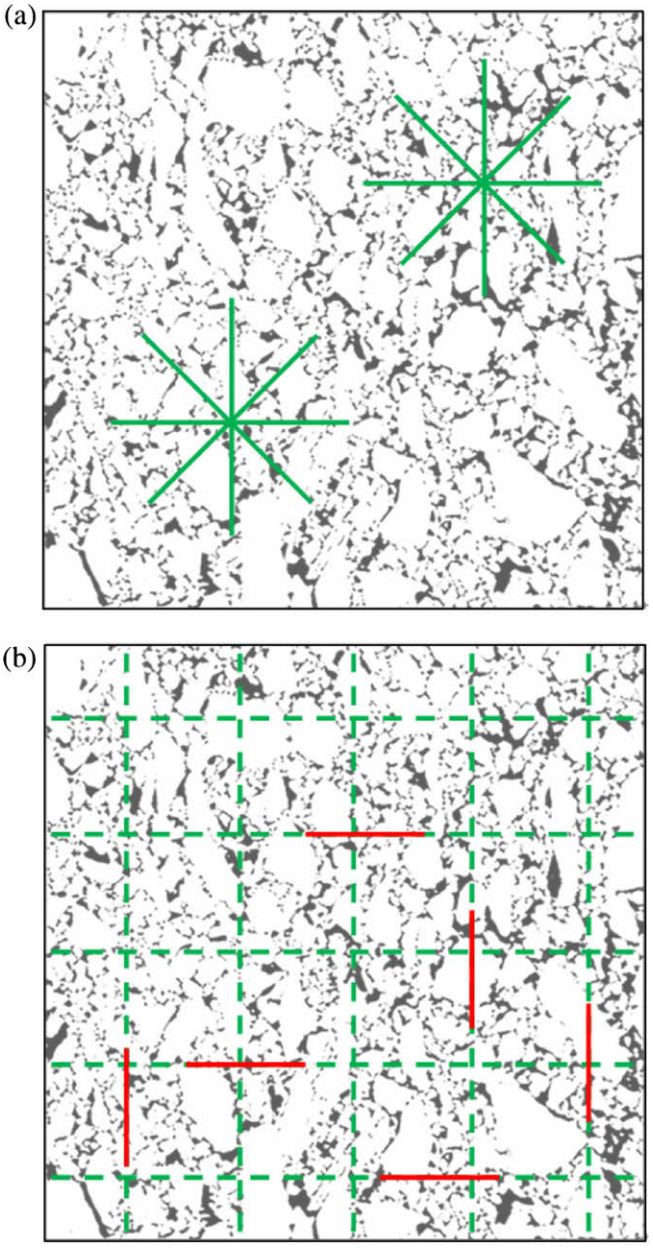

Fig. 2. Templates to compute two-point correlation functions: (a) radial template and (b) parallel-line template (black: coarse capillary pores detected in a BSE image).

3. Results and discussion

3.1. Visual comparison of images obtained by the SEM-BSE examination and the computer simulation

Fig. 3 shows a comparison of degrees of hydration of cement between the image analysis and the simulation. The simulated degree is much smaller than the degree directly obtained by the image analysis at an age of 1 day. However, difference in the degree of hydration is greatly reduced at 7 days. A little increase in the degree of hydration after 7 days is also represented in the simulation. The degrees of the simulation at 28 and 91 days are comparable to the ones obtained by the image analysis. It therefore seems that the simulation can represent the progress of hydration of cement at long ages.

BSE images and typical output of simulated structures at 1 and 7 days are shown in Fig. 4. Large continuous capillary pores with

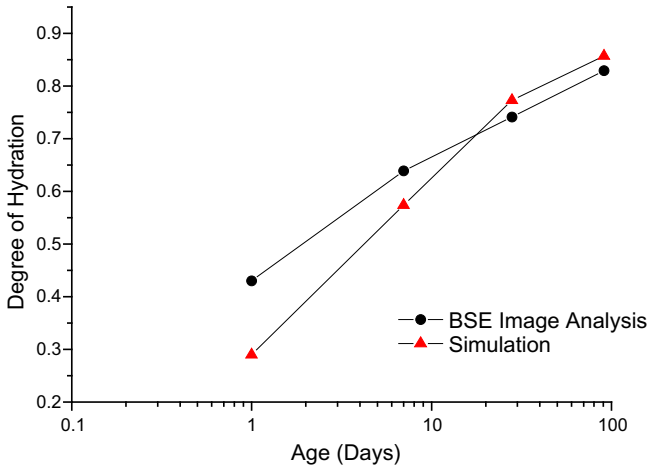

Fig. 3. Comparison of hydration degree as obtained by SEM-BSE examination and by simulation.

irregular shape are found in the image at 1 day (Fig. 4a), as expected from the small degree of hydration. In addition to these capillary pores, some Hadley particles are also found in the BSE images. On the other hand, the simulated structure which has a lower degree of hydration at 1 day, has little hydration product (Fig. 4b). Therefore, the phase of capillary pore is so continuous as to cover the whole 2-D region. Obviously, characteristics of capillary pore structure observed in the BSE image are not represented in the simulation for 1 day. At the age of 7 days, continuous phases of cement gel are formed to divide the continuous pore region into individual capillary pores, at least in two dimensions, as found in Fig. 4c. Such a segmentation of capillary regions is also found in the simulated structure at 7 days (Fig. 4d). The pore size in the simulated structure (Fig. 4d) varies from large to small as in the real structure. However, it appears that many capillary pores of one pixel (i.e. 1 μm^2) are uniformly dispersed in the whole region of the simulation output. Judging from only visual impression for the BSE images and the output map of the simulated structures at 7 days, one may have an impression that the simulated structure resembles the observed one of cement paste as a whole.

A comparison between BSE images and the simulated structures for longer ages of 28 and 91 days is given in Fig. 5. Dense structure with few visible pores is formed in the real cement pastes. Most of the areas are occupied by continuous solid phases (Fig. 5a and c). However, it should be noted that relatively large pores are still left in the cement pastes. As Diamond has pointed out [7], some of them have characteristics of the Hadley particle. As for the simulation, a random array of remnant cement particles is also observed in the simulated structure at the long ages. Such a manner of dispersion for the cement particles looks similar to the images. Namely, random distribution of unhydrated cement particles in the cement paste is represented in the simulation model.

Contrary to those cement particles, the simulated structure for capillary pores (Fig. 5b and d) is quite different from the observed one. There are many pores of one pixel in the simulation models for 28 and 91 days. They are almost uniformly dispersed in the complementary region to cement particles. Such a homogenous distribution of the pores of a uniform size is not observed in the real structure at those ages. The observed structure is more heterogeneous in size than the simulation output. It is clearly seen in Fig. 5 that there are visual differences in the pore structure between the model output and the observed microstructure.

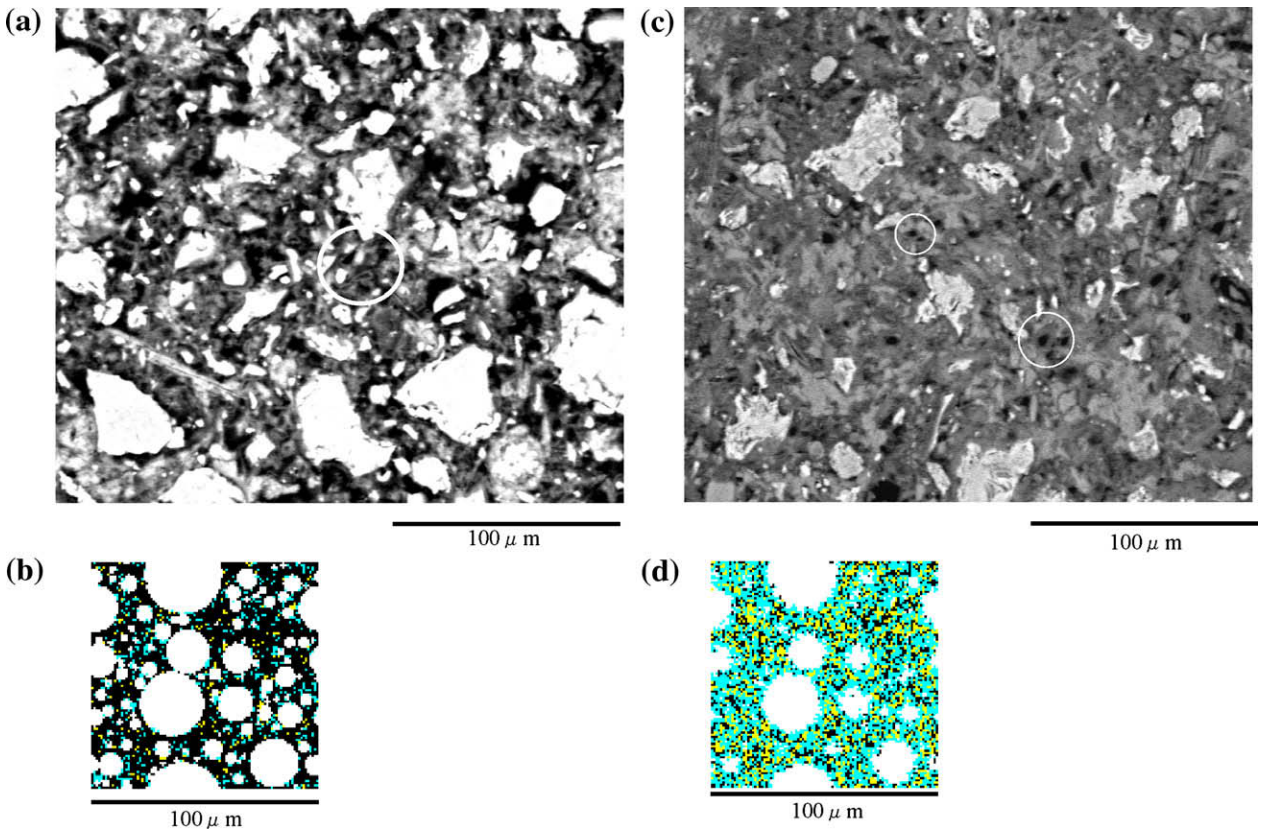

Fig. 4. Comparison for 1 day and 7 days-old cement pastes: (a) BSE image at 1 day (circled: examples of Hadley particles); (b) simulation output at 1 day (white: cement, blue: CSH, yellow: CH); (c) BSE image at 7 days; (d) simulation output at 7 days. (For interpretation of the references to colour in this figure legend, the reader is referred to the web version of this article.)

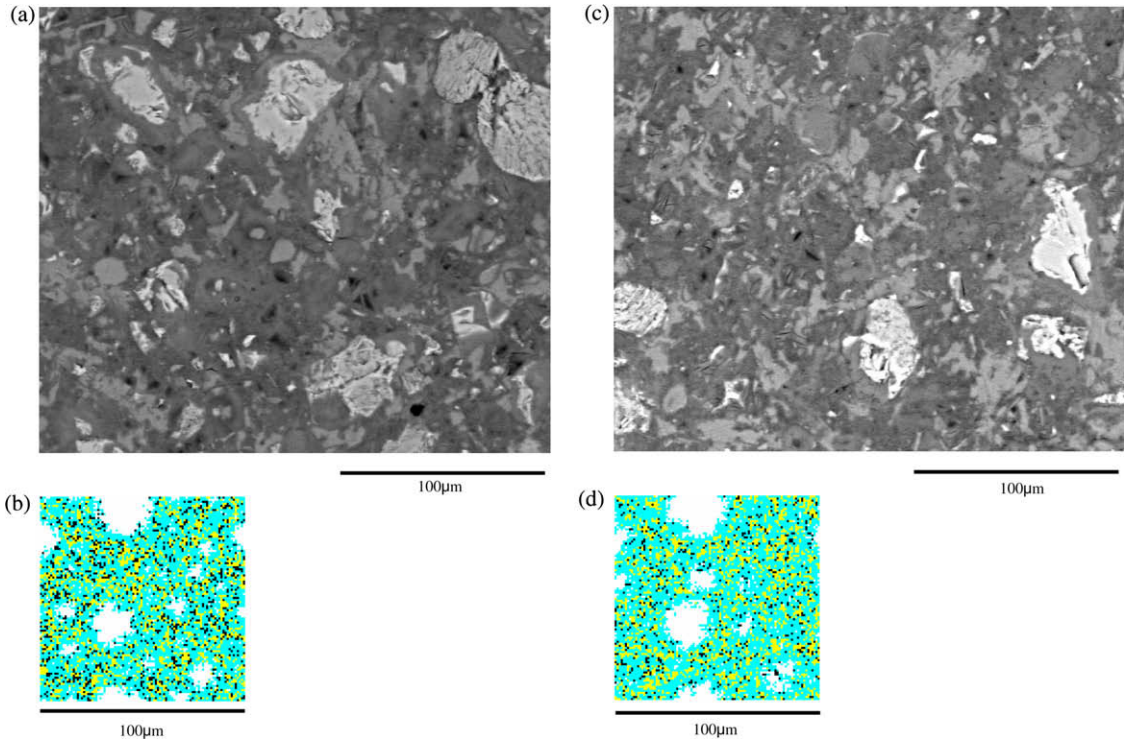

Fig. 5. Comparison for 28 days and 91 days-old cement pastes: (a) BSE image at 28 days; (b) simulation output at 28 days; (c) BSE image at 91 days; (d) simulation output at 91 days.

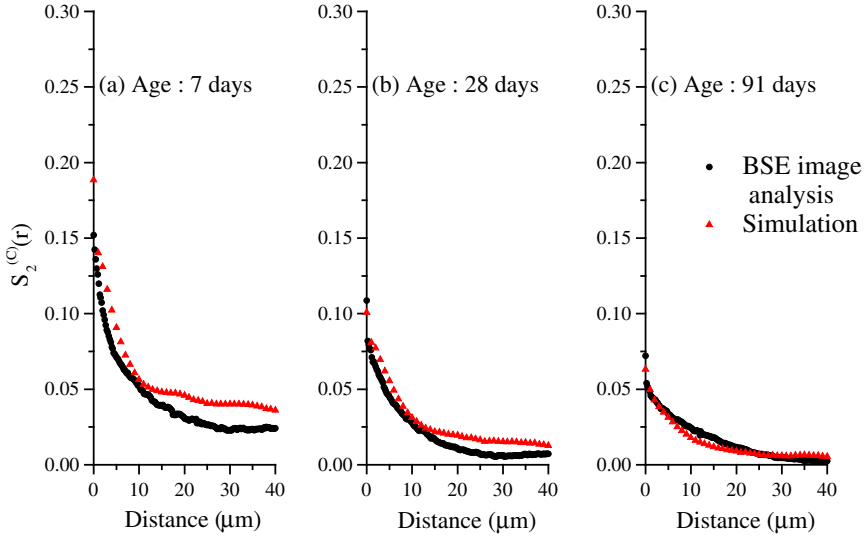

Fig. 6. Two-point correlation functions for unhydrated cement particles: (a) 7 days; (b) 28 days; (c) 91 days.

3.2. Quantitative comparison by two-point correlation functions

3.2.1. Spatial structure of cement particles

A comparison of the two-point correlation functions for unhydrated cement particles is shown in Fig. 6. The initial value of the function which corresponds to the volume fraction of cement in the simulated structure, is greater than the value for the BSE images at 7 days since the simulated degree of hydration is lower than the actual degree, as shown in Fig. 3. The function for the simulated structure is also greater than for the observed structure at long distances since the asymptotic value of the function is determined by the volume fraction squared. However, differences in the functions between observed and simulated structures decreased with time (Fig. 6b and c). At the long age of 91 days, there is little difference between the functions. Namely, spatial arrangement of the cement particles is well represented in the simulation model at long ages as a whole.

At the age of 7 days, the structure distance for the observed structure is around 30 μm. It is difficult to precisely determine the structure distance for the simulated structure at this age since the function still decreases gradually. It is around 40 μm in the simulation for the same age if the distance is determined solely

by the volume fraction squared. However, taking account of statistical artefacts that the function does not decline to the volume fraction squared in simulated data [20], the distance at which the gradient of function changes markedly is considered as the structure distance in the simulated structure. Then, the structure distance in the simulation model at 7 days is about 15–25 μm. This distance in the simulation is slightly smaller than the observed structure. The distance does not appreciably change in the simulated structure at longer ages whereas the structure distance increased with time in the observed structure. The increase in the distance results from a fine particle effect. Cement particles disappear from small to large as the hydration process proceeds. Furthermore, smaller particles have lower probability of appearance at a specific cross section. Such a fine particle effect is not well observed in the simulation output.

The distance is also related to the average 3-D size of the spatial structure. In other words, the size reflects the minimum necessary length to characterize a spatial structure with random heterogeneous nature. The smaller the size, the less elements are needed for describing the spatial structure. Therefore, the two-point function for cement indicates that the simulated structure with the smaller distance is more homogenous than the observed structure.

The lineal-path functions for the remnant cement in observed and simulated structures are shown in Fig. 7. The functions for observed structure are greater than the simulated structure. Furthermore, the distances that the functions decay to the horizontal axis are about 10–15 μm greater than in the simulated structure. This function fundamentally depends on the average size and shape of particles. Therefore, such a disagreement suggests that size and shape of residual cement particles are not well represented in the simulation model even when their spatial arrangement is similar to the structure in BSE images, as shown in Fig. 6.

Fig. 8 shows the normalized two-point correlation functions for cement particles. The functions given in Fig. 6 are normalized by their asymptotic values (the volume fraction squared), in order to eliminate the influence of difference in volume fractions on the functions. In the absence of any correlation between two points, their distribution is considered completely random (i.e. Poisson distribution). Then the probability is given by multiplying the probabilities (i.e. V_p^2). This is the reference value of 1.0 (a null-model) for comparing the structure in terms of spatial statistics. The normalized two-point function is essentially the same as pair correlation function for a point process [14]. The range in which the function is above the reference value means clustering tendency of cement pixels. On the contrary, the value lower than the reference value intuitively implies there is a gap between particles.

At the age of 7 days, clustering tendency than the Poisson distribution extends beyond 40 μm both in the observed and simulated structures. At longer ages, the simulated structure still exhibits the clustering tendency. However, the function for observed structure reduced below the reference at 28 and 91 days. Namely, in the observed structure, there are gaps of cement particles at longer distance of 20–30 μm. This fact suggests that the fine particle disappearance is more remarkable in the observed microstructure. As observed in Fig. 5, there are more particles of one pixel size in the whole region of the simulated structure. These lead to greater probability of positive correlation against the Poisson distribution.

3.2.2. Spatial structure of coarse capillary pores

Two-point functions for capillary pore phases are shown in Fig. 9. It should be noted that there is an essential difference in pores between BSE images and the simulation. The entire capillary porosity is expressed by pixels in the simulation, while only coarse capillary pores greater than the resolution of the image are taken into account to calculate the function for BSE images. Therefore, the range of pore sizes and the porosity are essentially different from each other. Due to those differences, there must be some differences in the initial values and the asymptotic values between the simulation and the observed structure since those characteristic values are determined by the porosity.

As expected, the function for the simulated structure at 7 days is much greater than the function obtained for the BSE images. The absolute difference in the functions between both structures is greatly reduced at longer ages. However, the asymptotic values of the function for the simulated structure continue to be greater than those for the observed structure since the total porosity represented in the simulation is always greater than the coarse capillary porosity that is observed in BSE images. At 91 days, the two-point function for the simulated structure is almost the same as that for the BSE structure except the initial values for the porosity.

The lineal-path functions for pores in observed and simulated structures are shown in Fig. 10. The initial value of the function for the simulated structure is far greater than for the observed structure because of difference in porosity, as mentioned above. If a length at which the function converges on the abscissa is defined as the maximum length, it is regarded as a possible length

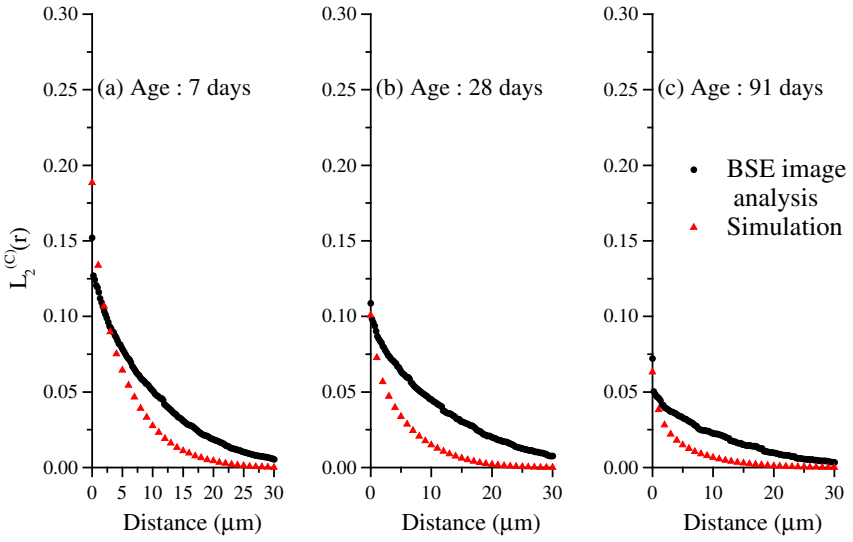

Fig. 7. Lineal-path functions for unhydrated cement particles: (a) 7 days; (b) 28 days; (c) 91 days.

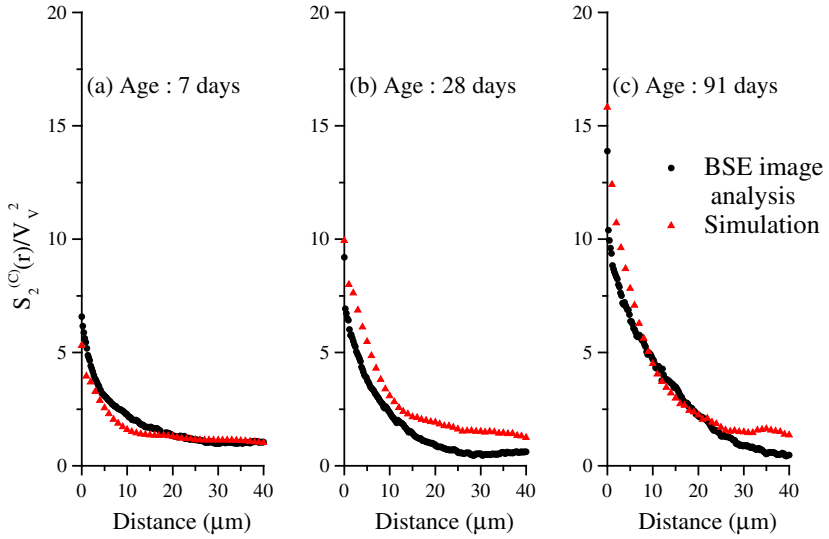

Fig. 8. Normalized two-point correlation functions for unhydrated cement particles: (a) 7 days; (b) 28 days; (c) 91 days.

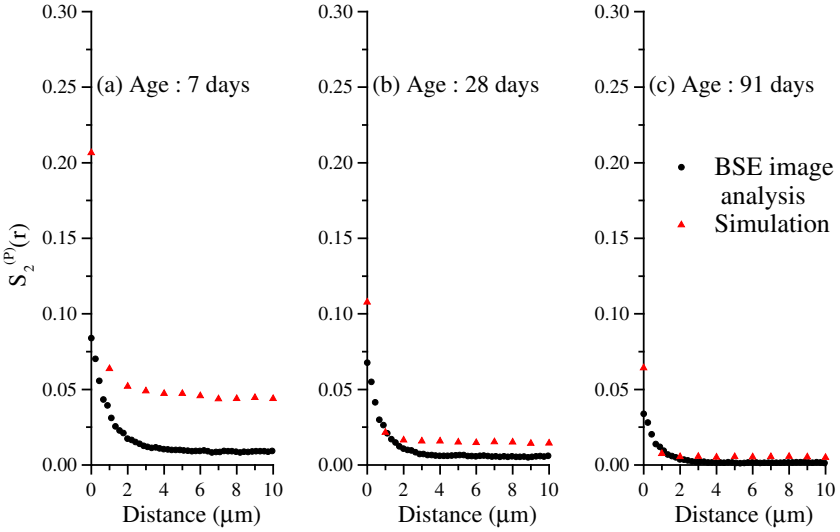

Fig. 9. Two-point correlation functions for capillary pores: (a) 7 days; (b) 28 days; (c) 91 days.

scale which reflects lineal continuity of a pore. The maximum length in the simulation is about 4–5 μm at 7 days. This is almost the same as the corresponding length of 5 μm in the observed structure. At the long ages, there is no difference in the length between the observed and simulated structures. This length can be related to the maximum size of pores with irregular shape in 2-D images. Actually, as found in Fig. 5 as well, the maximum size of visible pores in the BSE images is almost comparable with the size in the simulation output. Therefore, the maximum lineal continuity of large pores in mature pastes seems to be represented by the simulation.

Fig. 11 shows the normalized two-point correlation functions for the pores. Spatial distribution of capillary pores is quite different in the range of small distances between the observed and the simulated structures. The function of the observed structure is always greater than the simulated structure. The function for the simulated structure steeply drops at 1 μm. The pore distribution in the simulation output is almost Poisson beyond the distance of 1 μm while a region of clustering extends to about 4 μm in the BSE microstructure. This difference in clustering of pore pixels clearly results from incorrect size distribution of pores, as shown in Fig. 5. There are many pores of one pixel (i.e. 1 μm) which are directly surrounded by hydration products. However, there are few large pores consisting of some pixels in the simulation (Fig. 5). In other words, clustering tendency of pore pixels against the random distribution is not represented in the simulation. It is concluded that the spatial distribution of capillary pores in the model does not agree with the structure for coarse pores in BSE images.

3.3. Significance of comparison between real and simulated structures

It is clearly revealed by Figs. 6–11 that the UT version of CEMHYD3D simulation does not always correctly represent the observed structure with respect to visual impression and the statistical correlation functions for spatial structure. However, it should

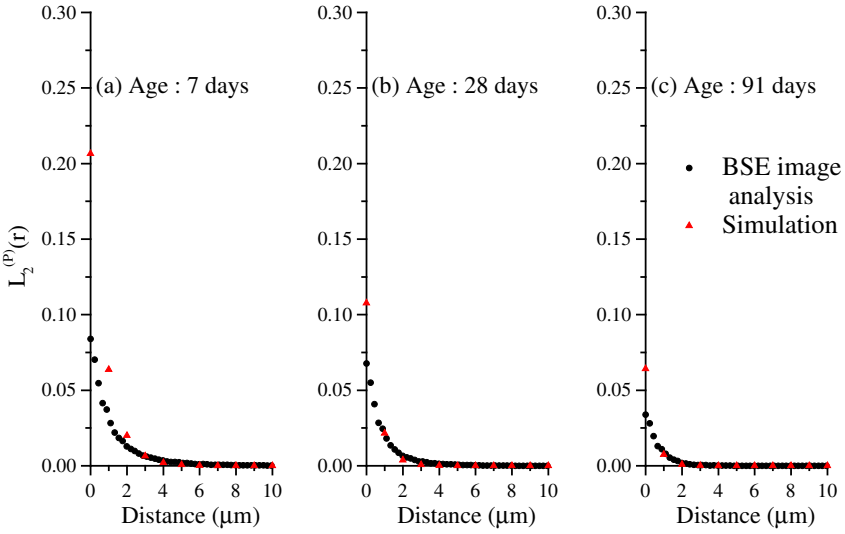

Fig. 10. Lineal-path functions for capillary pores: (a) 7 days; (b) 28 days; (c) 91 days.

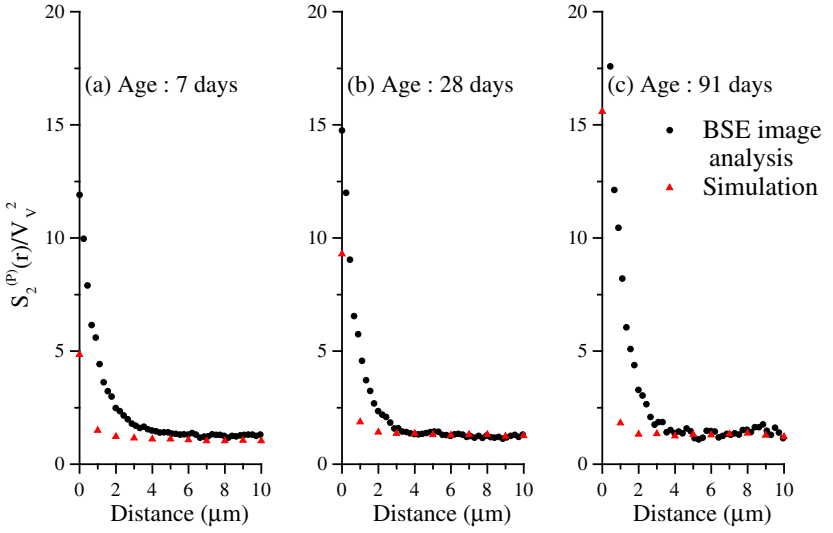

Fig. 11. Normalized two-point correlation functions for capillary pores: (a) 7 days; (b) 28 days; (c) 91 days.

be noted that such a disagreement especially in the pore structure is logically deduced. As schematically shown in Fig. 12, the total capillary porosity is represented in the simulation. The entire porosity is expressed by pixels with a specific size of 1 μm. Thus, pore space in pores of actual sizes less than 1 μm is included in the output as a part of the simulated total porosity. Therefore, the pore spaces are necessarily expressed in the output as pores of sizes of at least one pixel. Accordingly, the pore structures in the simulation model are virtual since there are no fine pores.

On the other hand, the structure in BSE images represents only the coarse pore structure, in which pores greater than the image resolution of 0.2 μm are detected in this study. Therefore, fine capillary pores less than the image resolution are not tallied in the image analysis. For example, using the Powers model [21] and the degree of hydration determined by the image analysis, the total capillary porosity of the cement paste at 28 days is approximately evaluated about 0.20 in this study [22]. The porosity detected in the BSE images is about 0.07, as found from Fig. 9b. Therefore, more than 50% of capillary pores in volume were missing in the BSE images. Consequently, comparison of the observed image with the simulation output is, in other words, to compare a part with the whole. As a result, pore structures represented by the image and the simulation must be different to each other in pore volume, size and location. In other words, second-order stereology has a part of its background in the spatial set theory. The subset of capillary pores must be different from its universal set of the total porosity.

It should be noted that this disagreement does not result from the difference in image resolution between the SEM examination and the simulation. Such a difference cannot be solved even when the same resolution is used between them. A more refined arrangement of pores could be generated by the simulation if it would be executed at the same resolution as the SEM examination (Fig. 12b). However, this still presents the same situation as in Fig. 12a. A part in the whole structure is compared with the total pore structure. It is logically impossible to establish a one-to-one mapping relation-

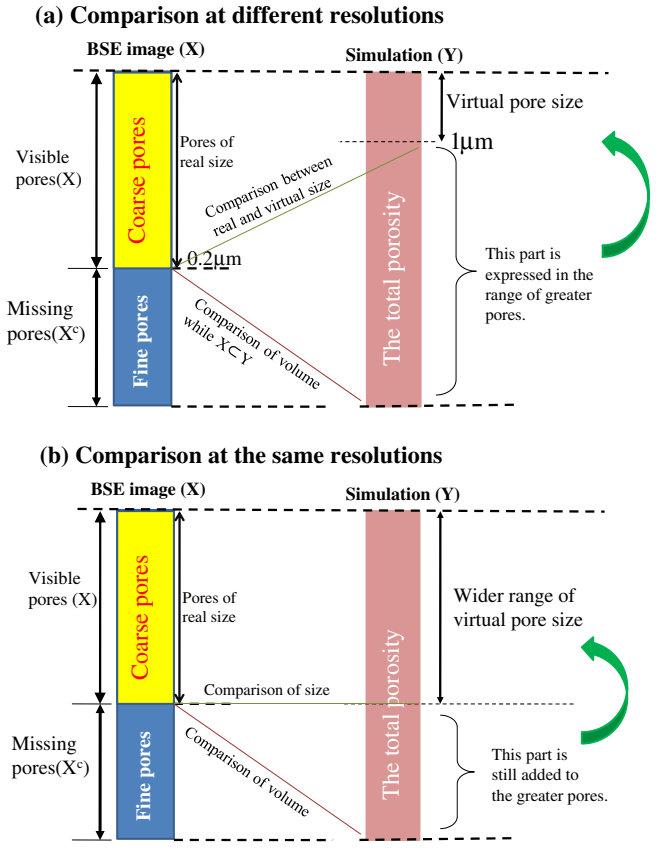

Fig. 12. Schematic drawing on inappropriate comparison of spatial structure between the SEM-BSE images (X) and the simulation model (Y) under condition of $X \subset Y$.

ship between the observed image and the simulation model as long as the subset is compared with the universal finite set. Therefore, if the simulation model structure can represent the real microstructure revealed by some images, then there must be little pore volume less than the visible pores in the images. Otherwise, only coarse pores as visible in the real SEM images must be correspondingly simulated by the model. Then, it is possible to establish the mapping relationship between two spatial finite sets of pores.

In order to confirm the validity of a simulation model, geometrical features in the simulation output should be compared with real images. The CEMHYD3D simulation is widely used and it may be regarded as a popular tool in computational materials science of concrete. In spite of being used widely, quantitative comparison of geometrical features between them seems to be rather seldom performed hitherto. There is an inclination to decide that the simulation output is truly representative of real structure, based on only a visual qualitative impression. However, as mentioned above, the simulation structure cannot be simply compared with observed microstructure of SEM-BSE images even if the simulation output seems very similar to the real image at a first glance.

For example, recent durability problems of concrete are greatly influenced by spatial structure of pores. Simulation could be useful and informative if the evolution of pore structure in cement pastes can be predicted in advance. However, it should be noted that finding an apparent agreement in microstructure between the CEMHYD3D simulation output and the real image of a certain magnification may not correctly address the problem on validity of the simulated structure in some cases. In other words, the validity of the CEMHYD3D simulation should be evaluated apart from the microstructure itself.

4. Conclusions

Geometrical features in the microstructure of cement pastes were quantitatively evaluated by the spatial correlation functions. The major results obtained in this study can be summarized as follows:

(1) The two-point function for cement particles in the CEMHYD3D simulated structure is almost the same as the function for the BSE image at long ages. Spatial structure of cement is well represented in the simulation model at long ages.
(2) The lineal-path and the normalized two-point functions for the cement particle in the simulated structure do not agree with the functions in the observed structure. This results from inadequate correspondence of average size and shape of cement particles.
(3) The distribution of large pores in the whole simulated capillary pore space looked similar to SEM-BSE images at the same age. However, geometrical features in the simulated pore structure were quite different from the coarse pore structure in the BSE images.
(4) The maximum lineal continuity of simulated pores is in agreement with the real coarse pores in cement pastes. However, the spatial arrangement of coarse pores in the observed structure does not correspond to the distribution of the pores in the simulated structure.
(5) The pores obtained from SEM-BSE images are elements of a subset, whereas the pores simulated by the CEMHYD3D model represent the whole of capillary porosity, i.e., the universal set. When the differences between the subset and universal set are not negligible, as would be the case in many conceivable examples, direct comparison of microstructures obtained from images and simulated by CEMHYD3D is not appropriate.

Acknowledgments

This study was carried out at the University of Twente within the framework of Bilateral Cooperation Programs between the Japan Society for the Promotion of Science (JSPS) and the Netherlands Organization for Scientific Research (NWO). The financial support from NWO and JSPS is acknowledged.

References

[1] Jennings H, Kropp J, Scrivener K, editors. The modelling of microstructure and its potential for studying transport properties and durability. Dordrecht: Kluwer Academic Publishers; 1996.
[2] van Breugel K. Numerical simulation of hydration and microstructural development in hardening cement-based materials (I) theory. Cem Concr Res 1995;25(2):319–31.
[3] Bentz DP. Three-dimensional computer simulation of portland cement hydration and microstructure development. J Am Ceram Soc 1998;80(1):3–21.
[4] Navi P, Pignat C. Three-dimensional characterization of the pore structure of a simulated cement paste. Cem Concr Res 1999;29(4):507–14.
[5] Maekawa K, Kishi T, Chaube RP, Ishida T. Coupled mass transport, hydration and structure formation theory for durability design of concrete structures. In: Proceedings of JCI symposium on chemical reaction and process analysis of cement concrete, JCI; 1996. p. 45–52 [in Japanese].
[6] Maekawa K, Ishida T, Kishi T. Multi-scale modeling of concrete performance-integrated material and structural mechanics. J Adv Concr Technol 2003;1(2):91–126.
[7] Diamond S. An "unmodel" of portland cement hydration. In: Proceedings of 2nd international symposium on advances in concrete through science and engineering. Quebec City, Canada; 2006. p. 15–29.
[8] Torquato S, Stell G. Microstructure of two-phase random media, the n-point probability functions. J Chem Phys 1982;77(4):2071–7.
[9] Bentz DP. Quantitative comparison of real and CEMHYD3D model microstructures using correlation functions. Cem Concr Res 2006;36(2):259–63.

[10] Japan Industrial Standards R5201: physical testing methods for cement; 1997.
[11] Wong HS, Head MK, Buenfeld NR. Pore segmentation of cement-based materials from backscattered electron images. Cem Concr Res 2006;36: 1083–90.
[12] Mindess S, Young JF, Darwin D. Concrete. 2nd ed. Upper Saddle River: Prentice Hall; 2003.
[13] Takagi M, Shimoda H, editors. Handbook of image analysis (revised edition). Tokyo: University of Tokyo Press; 2004 [in Japanese].
[14] Howard CV, Reed MG. Unbiased stereology, three-dimensional measurement in microscopy. 2nd ed. Oxon, UK: BIOS Scientific Publishers; 2005.
[15] Kjellsen KO, Fjallberg L. Measurements of the degree of hydration of cement paste by SEM, ^{29}Si NMR and XRD methods. In: Proceedings of workshop on water in cement paste and concrete, hydration and pore structure. Skagen, Denmark: The Nordic Concrete Federation; 1999. p. 85–98.
[16] Bentz DP, Stutzman PE. Curing, hydration, and microstructure of cement paste. ACI Mater J 2006;103(5):348–56.
[17] Chen W. Hydration of slag cement: theory, modelling and application. PhD thesis, University of Twente, 25 January 2007. Enschede, The Netherlands; 2007.
[18] Chen W, Brouwers HJH, Shui ZH. Three-dimensional computer modeling of slag cement hydration. J Mater Sci 2007;42(23):9595–610.
[19] Chen W, Brouwers HJH. Mitigating the effects of system resolution on computer simulation of Portland cement hydration. Cem Concr Compos 2008;30(9):779–87.
[20] Mattfeldt T, Stoyan D. Improved estimation of the pair correlation function of random sets. J Microsc 2000;200(2):158–73.
[21] Powers TC, Brownyard TL. Studies of the physical properties of hardened Portland cement paste, Bull. 22, Res. Lab. of Portland Cement Association, Skokie, IL, U.S.A. Reprinted from: J. Am. Concr. Inst. (Proc.) 1947;43:101–32, 249–336, 469–505, 549–602, 669–712, 845–80, 933–92.
[22] Igarashi S, Kawamura M, Watanabe A. Analysis of cement pastes and mortars by a combination of backscatter-based SEM image analysis and calculation based on the Powers model. Cem Concr Compos 2004;26(8):977–85.